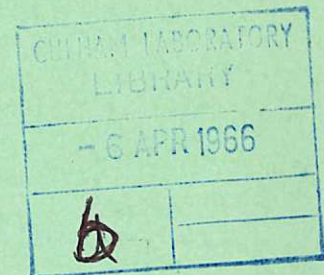


This document is intended for publication in a journal, and is made available on the understanding that extracts or references will not be published prior to publication of the original, without the consent of the author.



United Kingdom Atomic Energy Authority

RESEARCH GROUP

Preprint

A calculation of the intensities of
optically thick lines emitted by
hydrogen-like ions in a steady-state plasma

A. G. HEARN

Culham Laboratory,
Culham, Abingdon, Berkshire

1966

© - UNITED KINGDOM ATOMIC ENERGY AUTHORITY - 1966
Enquiries about copyright and reproduction should be addressed to the
Librarian, Culham Laboratory, Culham, Abingdon, Berkshire, England.

Culham Laboratory
Culham, Abingdon, Berkshire
1966

UNCLASSIFIED

CLM - P 97

(Approved for publication)

A CALCULATION OF THE INTENSITIES OF OPTICALLY THICK LINES
EMITTED BY HYDROGEN-LIKE IONS IN A STEADY-STATE PLASMA

by

A.G. HEARN

(Submitted for publication in Proc. Phys. Soc.)

U.K.A.E.A. Research Group,
Culham Laboratory,
Nr. Abingdon,
Berks.

January, 1966 (ED)

A B S T R A C T

The intensities of optically thick lines emitted by hydrogen-like ions in a plasma which is in a steady state have been calculated for electron temperatures between $8000 Z^2 \text{ }^\circ\text{K}$ and $256000 Z^2 \text{ }^\circ\text{K}$ and for electron densities between $10^8 Z^7 \text{ cm}^{-3}$ and $10^{18} Z^7 \text{ cm}^{-3}$, where Z is the charge of the bare nucleus. The optical thickness of the plasma, which is conveniently measured at the centre of the Lyman α line, is between 0.1 and 100 for a uniform plane parallel plasma. The calculations solve the coupled equations of transfer when necessary for the first twenty levels for the absorption and stimulated emission of photons in the lines and include the processes of excitation, de-excitation and ionization by electron collision, spontaneous radiative decay, three-body recombination and radiative recombination. It is assumed that the ratio of the electron density to the bare ion density is constant through the plasma. It is also assumed that all the lines are Doppler broadened and that the plasma is optically thin for the continuum.

Tables give the total intensity of the Lyman α and β lines and the Balmer α and β lines, the total power radiated in the lines from both sides of the plasma and the geometrical size of the plasma. The population density of the ground level is given when this is not very small compared with the electron density.

C O N T E N T S

	<u>Page</u>
1. INTRODUCTION	1
2. THE ATOMIC PROCESSES	2
3. SOLUTION OF THE EQUATION OF TRANSFER	4
4. THE METHOD OF SOLUTION	9
5. THE RESULTS	12
6. DISCUSSION OF THE RESULTS	28
ACKNOWLEDGEMENTS	31
REFERENCES	31

1. INTRODUCTION

The combined effect of collisional and radiative processes in an optically thin hydrogen and hydrogen-like ion plasma has been studied in a number of papers. Bates, Kingston and McWhirter (1962) showed that for moderate electron densities the rate of three-body recombination to high bound levels followed by collisional de-excitation and spontaneous decay can be much greater than the rate of radiative recombination directly to the ground level; and that the rate of excitation from the ground level to an excited level followed by ionization can be greater than the rate of collisional ionization directly from the ground level.

Similarly, these processes are important in determining the populations of the excited levels and hence the intensities of the lines emitted by the plasma. Bates and Kingston (1963) and McWhirter and Hearn (1963) showed that in an optically thin plasma which is not in a steady state, the excited levels may be specified by the instantaneous population density of the ground level for a given electron temperature and density and, since the equations are linear, the variation of an excited level population density with the ground level population density may be represented by two coefficients.

This paper extends the calculations of McWhirter and Hearn to an optically thick plasma by including photo-excitation and stimulated emission in all the line radiation. The difficulty of the calculation increases with the total optical thickness of the plasma, which is conveniently measured at the centre of the Lyman α line, and the methods used here give reasonable accuracy only for optical thicknesses in Lyman α up to 100. For such modest thicknesses photo-ionization is negligible. The inclusion of photo-excitation terms, particularly between excited levels, makes the equations non-linear. Consequently it is not possible to represent the population densities for a transient plasma in any simple way, and the line intensities are given only for a plasma in a steady state.

The solution of the equation of transfer for the line radiation depends on the geometry of the plasma and it is solved for a plane parallel plasma of finite

thickness having a constant electron density and temperature assuming pure doppler broadening. It is also assumed that all radiation originates in the plasma and that there is no external source of radiation.

2. THE ATOMIC PROCESSES

These calculations include photo-excitation and stimulated emission as well as all the collisional and radiative processes in the optically thin calculation of McWhirter and Hearn (1963). Photo-ionization is still not included.

The rate coefficients for excitation by electron impact from level p to level q , $K(p,q)$ and its inverse $K(q,p)$, those for ionization from level p by electron impact $K(p,c)$ and its inverse $K(c,p)$ and those for radiative recombination are exactly as discussed by McWhirter and Hearn (1963).

The other processes included in the calculation are spontaneous radiative decay from level p to level q and its inverse of photo-excitation.

$$N^{(z-1)+}(p) \rightleftharpoons N^{(z-1)+}(q) + h\nu \quad \dots (1)$$

and stimulated emission from level p to level q

$$N^{(z-1)+}(p) + h\nu \rightarrow N^{(z-1)+}(q) + h\nu + h\nu \quad \dots (2)$$

The spontaneous transition probability is given by the Einstein coefficient $A(p,q) \text{ sec}^{-1}$. The rate coefficient for photo-excitation is

$$\frac{B(q,p)}{\Delta\nu_D \sqrt{\pi}} \int_0^\infty \rho_\nu e^{-\left(\frac{\nu - \nu_0}{\Delta\nu_D}\right)^2} d\nu \text{ sec}^{-1} \quad \dots (3)$$

where the radiation density ρ_ν at the frequency ν is integrated over the doppler broadened absorption profile for the line centred at the frequency ν_0 and whose e^{-1} width is $\Delta\nu_D$. $B(q,p)$ is the Einstein absorption coefficient.

The rate coefficient for stimulated emission is

$$\frac{B(p,q)}{\Delta\nu_D \sqrt{\pi}} \int_0^{\infty} \rho_\nu e^{-\left(\frac{\nu - \nu_0}{\Delta\nu_D}\right)^2} d\nu \text{ sec}^{-1} \quad \dots (4)$$

The Einstein coefficient $B(p,q)$ for stimulated emission is related to the absorption coefficient $B(q,p)$.

$$\omega(p) B(p,q) = \omega(q) B(q,p) \quad \dots (5)$$

where $\omega(p)$ is the statistical weight of the p th level.

It is assumed throughout that the free electrons have a Maxwellian distribution and that the sub-states of a level are populated according to their statistical weight. This assumption may not be valid for some of the low excited levels at low densities.

The rate of change of the population density $n(p)$ for level p is given by

$$\begin{aligned} \frac{dn(p)}{dt} = & - n(p) \left\{ n(c) \left[K(p,c) + \sum_{q \neq p} K(p,q) \right] \right. \\ & + \sum_{q < p} A(p,q) + \sum_{q > p} \frac{B(p,q)}{\Delta\nu_D \sqrt{\pi}} \left(1 - \frac{\omega(p)n(q)}{\omega(q)n(p)} \int_0^{\infty} \rho_\nu e^{-\left(\frac{\nu - \nu_0}{\Delta\nu_D}\right)^2} d\nu \right) \left. \right\} \\ & + n(c) \sum_{q \neq p} n(q) K(q,p) + \sum_{q > p} n(q) A(q,p) \\ & + \sum_{q < p} \frac{n(q) B(q,p)}{\Delta\nu_D \sqrt{\pi}} \left(1 - \frac{\omega(q)n(p)}{\omega(p)n(q)} \int_0^{\infty} \rho_\nu e^{-\left(\frac{\nu - \nu_0}{\Delta\nu_D}\right)^2} d\nu \right) \\ & + \frac{n(c)^2}{X} \left[K(c,p) + \beta(p) \right] \quad \dots (6) \end{aligned}$$

where $n(c)$ is the number density of the free electrons and X is the ratio of $n(c)$ to the number density of bare nuclei of charge Z .

There are an infinite number of these equations, one for each bound level. For the steady state solution the left hand side is always zero.

For an optically thin plasma of uniform electron density and temperature the

coefficients of these equations are linear and independent of space. In an optically thick plasma the rate coefficients for photo-excitation and stimulated emission depend on the radiation density, which varies in space even in a uniform plasma, so that the equations for the rate of change of the population densities become a function of space. The radiation density has to be calculated by integrating, over all solid angles, the intensities obtained by solving the equation of transfer through the plasma. Since this depends on the population densities at other points in space the equations for the rate of change of population densities at one point in space are coupled to the equations at all other points. In addition to these complications the equations in general become non-linear in an optically thick plasma.

3. SOLUTION OF THE EQUATION OF TRANSFER

Using the definitions and nomenclature of Ambartsumyan (1958 Chapter 2) the equation of transfer is

$$\frac{dI_{\nu}}{ds} = - I_{\nu} \chi_{\nu} \rho + j_{\nu} \rho \quad \dots (7)$$

where I_{ν} is the specific intensity at the frequency ν , ρ is the mass density, ds is an element of geometrical distance, χ_{ν} is the absorption coefficient and j_{ν} is the emission coefficient. The emission and absorption coefficients may be redefined so that the stimulated emission term is included in the absorption term.

Then

$$j_{\nu} = \frac{n(p)h\nu_0}{\Delta\nu_D \sqrt{\pi}} \frac{A(p,q)}{4\pi} e^{-\left(\frac{\nu - \nu_0}{\Delta\nu_D}\right)^2} \quad \dots (8)$$

$$\chi_{\nu} = \frac{n(q)h\nu_0 B(q,p)}{\Delta\nu_D \rho c \sqrt{\pi}} \left[1 - \frac{\omega(q)n(p)}{\omega(p)n(q)} \right] e^{-\left(\frac{\nu - \nu_0}{\Delta\nu_D}\right)^2} \quad \dots (9)$$

and the source function, the ratio of the emission coefficient to the absorption coefficient, becomes

$$f = \frac{j_{\nu}}{\chi_{\nu}} = \frac{\frac{c n(p) A(p,q)}{4\pi n(q) B(q,p)}}{\left[1 - \frac{n(p)\omega(q)}{n(q)\omega(p)} \right]} \quad \dots (10)$$

and the element of optical depth $d\tau_\nu$ must be defined as

$$d\tau_\nu = \rho \chi_\nu \left[1 - \frac{n(p)\omega(q)}{n(q)\omega(p)} \right] ds \quad \dots (11)$$

It is assumed in these calculations that the source function varies only in space. Detailed numerical solutions of the equation of transfer have been made for a two level atom (Hearn 1963, 1964a) which show that for pure doppler broadening the assumption of a source function independent of frequency and angle is a very good one. In order to solve the equation of transfer, the variation of the source function in space must be represented in some way. The most efficient method used in the calculations for a two level atom expressed the variation of the source function in terms of an expansion of Chebyshev polynomials. The order of the expansion necessary to obtain good accuracy increases rapidly with the total optical thickness of the plasma. For an optical depth of 1000 it is necessary to use a 20th order polynomial. If a lower order polynomial is used the fractional error caused in the line profile is greater than the fractional error in the total line intensity. The variation of the source function is greatest at low electron densities where the source function at all points is much smaller than the black body value of the source function. As the electron density increases, the contribution to the source function from collisions dominates the radiative contribution and the source function becomes independent of position. To estimate the accuracy of using a low order polynomial for the source function, the total line intensity for a two level atom in a low electron density plasma was calculated using only a few terms in the Chebyshev expansion and compared with the accurate high order solution. The total line intensity expressed as a ratio of the intensity calculated from the 20th degree polynomial is shown in Fig.1 for zeroth, second and fourth degree polynomials plotted against the total optical depth of the plasma measured at the centre of the absorption profile. Only even polynomials are used because the source function is an even function of space. The improvement in accuracy obtained by changing from a zeroth degree to a quadratic approximation is large and for optical depths of 10 or less the quadratic solution is accurate to a few percent. For

optical depths of 100 the error of the quadratic solution has increased to 30% which would be adequate for many purposes considering the uncertainties of cross-section calculations. A further improvement in accuracy is obtained from a quartic approximation, but the increase in complexity in the calculation for a many level atom is very great. For comparison the total line intensity calculated using Holstein's solution is included in Fig.1.

Holstein (1947, 1951) represents the effect of photo-excitation by reducing the spontaneous emission probability by a fractional factor g which is calculated for a decaying plasma in a given geometry using the Rayleigh-Ritz variational method. In a decaying plasma where there is no internal source of excitation the imprisonment factor g becomes independent of space after the plasma has been decaying for a sufficiently long time. For a finite plane parallel plasma of total optical thickness τ , Holstein finds that the imprisonment factor is given by

$$g = \frac{1.06}{\tau(\log_e \tau/2)^{1/2}} \quad \dots (12)$$

In an optically thick plasma composed of two level atoms where excitation is maintained by collisional excitation, the excited level population is determined by the balance of the populating and depopulating processes so that

$$\frac{n(2)}{n(1)} = \frac{n(c) K(1,2)}{n(c) K(2,1) + g A(2,1)} \quad \dots (13)$$

The effect of photo-excitation is included by means of the imprisonment factor g which is now a function of space. Holstein's theory gives no information about its variation so it is assumed to be constant and equal to the value obtained for a decaying plasma.

The equation of transfer was solved through the plasma and the intensity integrated numerically to obtain the total line intensity which is shown in Fig.1 expressed as a ratio of the 20th degree Chebyshev solution.

The calculation of the source function using an n th degree polynomial approximation involves calculating the source function at $n+1$ points in space through

which the polynomial may be drawn. When the plasma is symmetrical, the points are duplicated and there are only $\frac{n}{2} + 1$ distinct points to be calculated. For a Chebyshev polynomial the points are conveniently situated at the zeros of the $n + 1$ th degree Chebyshev polynomial. When a quadratic approximation is used for the source function it is much more convenient to choose points at the centre and edge of the plasma.

This means that the set of equations (6) has to be calculated at the centre and edge to give the population densities and hence the source functions. A quadratic may be drawn through the values of the source functions, and the equation of transfer solved to give the intensities at the two points which can then be integrated over angle and frequency to give the rate of photo-excitation in that line. This may be repeated for as many lines as necessary.

The equation of transfer for a specific intensity I at a dimensionless frequency x at an angle θ to the outgoing normal of the plasma at a point whose optical depth τ is measured at the centre of the line along the normal from a given edge of the plasma is

$$\frac{\cos\theta}{e^{-x^2}} \frac{dI}{d\tau}(x, \theta, \tau) = -I(x, \theta, \tau) + f(\tau) \quad \dots (14)$$

Where f is the source function, a function of position only, and the dimensionless frequency x is

$$x = \frac{\nu - \nu_0}{\Delta\nu_D} \quad \dots (15)$$

for the particular transition.

If the source function is assumed to vary quadratically when measured from one edge of the plasma then

$$f(\tau) = b_1 + b_2 \tau + b_3 \tau^2 \quad \dots (16)$$

The substitution

$$a = \frac{e^{-x^2}}{|\cos \theta|} \quad \dots (17)$$

gives the equation of transfer the solution

$$\begin{aligned}
 I(x, \theta, \tau) &= e^{-a\tau} \int_0^{\tau} a(b_1 + b_2 \tau' + b_3 \tau'^2) e^{a\tau'} d\tau' \\
 &= b_1 + b_2 \left(\tau - \frac{1}{a}\right) + b_3 \left(\tau^2 - \frac{2\tau}{a} + \frac{2}{a^2}\right) \dots (18) \\
 &- e^{-a\tau} \left(b_1 - \frac{b_2}{a} + \frac{2b_3}{a^2}\right)
 \end{aligned}$$

The radiation density $\rho(x, \tau)$ at a given frequency is obtained by integrating the intensity over all solid angles. Because of the symmetry of the plane parallel geometry, the contribution ρ_p to the radiation density from one hemisphere is

$$\begin{aligned}
 \rho_p(x, \tau) &= \frac{1}{c} \int_0^{2\pi} I(x, \theta, \tau) d\omega \\
 &= \frac{2\pi}{c} \int_0^{\pi/2} I(x, \theta, \tau) \sin \theta d\theta \dots (19)
 \end{aligned}$$

and the contribution from the other hemisphere is given by $\rho_p(x, \tau_0 - \tau)$ where τ_0 is the total optical thickness of the plasma.

Thus

$$\begin{aligned}
 \rho_p(x, \tau) &= \frac{2\pi}{c} \left\{ b_1 + b_2 \left[\tau - \frac{1}{2e^{-x^2}} \right] + b_3 \left[\tau^2 - \frac{\tau}{e^{-x^2}} + \frac{2}{3e^{-x^2}} \right] \right\} \\
 &- \frac{2\pi}{c} \left[b_1 E_2(\tau e^{-x^2}) - \frac{b_2}{e^{-x^2}} E_3(\tau e^{-x^2}) + \frac{2b_3}{e^{-2x^2}} E_4(\tau e^{-x^2}) \right] \dots (20)
 \end{aligned}$$

where $E_n(t)$ the n th exponential integral of t is given by

$$E_n(t) = \int_1^{\infty} \frac{e^{-ty}}{y^n} dy \dots (21)$$

When τe^{-x^2} is small this expression suffers from severe cancelling and it is necessary to expand the exponentials before integrating, which gives

$$\begin{aligned} \rho_p(x, \tau) = \frac{2\pi}{c} \left\{ \tau e^{-x^2} b_1 \left[1 + E_1(\tau e^{-x^2}) \right] \right. \\ + b_2 \left[\frac{\tau^2 e^{-x^2}}{2} E_1(\tau e^{-x^2}) + \frac{3}{4} \tau^2 e^{-x^2} \right] \\ \left. + b_3 \left[\frac{11}{18} \tau^3 e^{-x^2} + \frac{\tau^3 e^{-x^2}}{3} E_1(\tau e^{-x^2}) \right] \right\} \quad \dots (22) \end{aligned}$$

This form was used for all τe^{-x^2} less than 0.1. To obtain the rate of photo-excitation the radiation density has to be multiplied by the absorption profile and integrated over frequency. This integration was done numerically using trapezoidal quadrature with seven points over half the profile spaced equally at units of 0.5 in x . The detailed two level calculations show that this quadrature is accurate if the optical depth is 100 or less.

4. THE METHOD OF SOLUTION

The assumption of a quadratic variation of the source function for the solution of the equation of transfer in the emission lines means that equation (6) has to be solved for all bound levels at two points in space.

As in the optically thin calculation, the solution of the equations for an infinite set of bound levels was avoided by assuming that level 20 and above have a Saha-Boltzmann population which is given by

$$n_E(p) = \frac{n(c)^2}{X} p^2 \left(\frac{h^2}{2\pi m k T_e} \right)^{3/2} \exp \left(\frac{E(p, c)}{k T_e} \right) \quad \dots (23)$$

where $n_E(p)$ is the Saha-Boltzmann population of level p , T_e is the electron temperature, m is the mass of the electron and $E(p, c)$ is the ionization potential of level p .

This assumption is valid for an optically thick plasma in all regions where it is valid for an optically thin plasma, since the inclusion of photo-excitation

provides the inverse process to spontaneous radiative transitions and this must make the populations tend to a Saha-Boltzmann population more rapidly than in an optically thin plasma.

The contribution to lower levels from levels above level 20 was included using the asymptotic value of the oscillator strength for the rate coefficients. The calculation assumed that the high levels remained discrete and successive levels were included until the contribution of the last level was less than 0.1% of the total for the levels already calculated.

The inclusion of the equation of transfer makes the equations non-linear. This non-linearity comes from the solution of the equation of transfer between two excited levels since the optical depth required in the calculation depends on the population densities of the lower level. The non-linearity in the equations means that an iterative method of solution is necessary at some stage. The equation of transfer has notoriously slow convergence in iteration and because of this slow convergence it is necessary to find a better starting value than the Saha-Boltzmann population. A comparison of the density of the excited level population for a two level atom obtained using Holstein's theory with the detailed numerical solution (Hearn 1963) shows that Holstein's theory is quite accurate for calculating the excited level population density at the centre of the plasma. Since the application of Holstein's theory to only the Lyman lines yields a linear set of equations, a starting value of the population density for each bound level was obtained by solving the equations modified in the spontaneous transition probabilities by the Holstein g factor using the Gauss pivotal condensation method.

The full solution was then obtained using a Gauss-Seidel iteration including the non-linear terms introduced by the solution of the equation of transfer between the excited levels. The equation of transfer between any two bound levels lower than 20 was solved if it was significant. The Gauss-Seidel iteration is concerned with balancing the rates of electrons into and out of the level. Photo-excitation into a level from a lower level was neglected if it was less than 1% of the rate

of collisional excitation into the level from the same lower level. This is the only other process transferring electrons between the two levels. This criterion is certainly satisfied if

$$0.01 n(c) k(q,p) \geq \frac{1}{\sqrt{\pi}} B(q,p) \int_{-\infty}^{+\infty} \rho_x e^{-x^2} dx \quad \dots (24)$$

The source function f for the transition is always greater at the centre than at the edge so that

$$\begin{aligned} \rho_x &\leq \frac{4\pi}{c} f_{\text{centre}} \left[1 - E_2(\tau e^{-x^2}) \right] \\ &\leq \frac{4\pi}{c} f_{\text{centre}} \end{aligned} \quad \dots (25)$$

and hence using the relation for the source functions

$$\frac{1}{\sqrt{\pi}} \int_{-\infty}^{+\infty} \rho_x e^{-x^2} dx \leq \frac{A(p,q)}{B(q,p)} \left[\frac{n(p)}{n(q)} \right]_{\text{centre}} \quad \dots (26)$$

Thus the criterion used for neglecting photo-excitation from level q into level p is

$$0.01 n(c) k(q,p) \geq A(p,q) \left[\frac{n(p)}{n(q)} \right]_{\text{centre}} \quad \dots (27)$$

Photo-excitation out of a level may be neglected if it is small compared with the total rate of all processes depopulating the level, and photo-excitation out of a level was neglected if it was less than 1% of the total depopulating rate. In all cases the contribution of photo-excitation out of the level to level 20 satisfied this criterion and no calculation of photo-excitation was made to higher levels.

In some cases the Holstein treatment in the Lyman lines does not give a good starting value for the ground level population density which is affected significantly by the introduction of the equation of transfer in the Balmer α transition. The reason for this will be discussed later. Under these circumstances the convergence is slow particularly for an optical depth in Lyman α of 100. The reason

for this slow convergence may be discussed in physical terms. At large optical depths in Lyman α the ground level and the first excited level are very closely coupled together by spontaneous transitions from the excited level and by photo-excitation from the ground level. The rates of these processes are very much greater than any other process populating the two levels so that there is a very large current of electrons circulating from level 1 up to level 2 and back again. Yet this circulation has little effect in determining the population density of the ground level which is determined by the much looser coupling through higher excited levels to the continuum. The convergence of the iteration may be increased by a factor of ten by subtracting the component circulating round the two lowest levels and using only the net rate of transfer in the calculations. This may be done simply in the Gauss-Seidel iteration by not including the Lyman α photo-excitation rate in the calculation of the increment of the ground level population from the total rate of processes depopulating the level. Since this process dominates all others the actual step per iteration is increased.

The close coupling between the ground level and level 2 rendered the standard methods of accelerating convergence such as the Aitken δ^2 acceleration or methods of solution based on the Newton Raphson process useless.

The early iterations starting from a constant population density across the plasma obtained from the Holstein solution were mainly concerned with establishing the spatial variation of the ground level population density rather than altering its general level. It was found that when convergence was speeded up by allowing for the circulation between the two lowest levels the iteration would overshoot badly. It was most convenient to apply the faster method of solution only after five or ten iterations when the main spatial variation of the population densities had been established.

5. THE RESULTS

The population densities for the first twenty bound levels at the edge and the centre of the plasma were calculated for a specified electron temperature and

density and optical depth at the centre of the Lyman α line for an ionic charge Z of one. The results for other values of the ionic charge may be obtained by scaling laws.

From these population density distributions the total line intensity emitted perpendicular to the plane of the plasma was calculated for the Lyman, Balmer and Paschen lines up to level 20 together with the total power radiated from both sides of a one square centimetre column of the plasma in Lyman α and in the whole Lyman, Balmer and Paschen series.

The population density distribution of the excited levels determines the optical depth in the line to the next higher level, and the ground level population density determines the geometrical thickness of the plasma since the optical depth in Lyman α is specified for the calculation.

The total line intensity is calculated from the solution of the equation of transfer for a quadratically varying source function by integrating equation (18) numerically over frequency. To obtain the total power loss from the surface, equation (18) must be integrated over all angles and frequencies. This was doubled to account for both sides of the plasma.

When the population density is assumed to vary quadratically then from equation (11) the optical depth $\tau(p,q)$ of the plasma at the centre frequency ν_0 of a transition between level q and level p not including the modification in the optical depth for stimulated emission is

$$\tau(q,p) = h \sqrt{\frac{m_i}{2\pi k T_i}} B(q,p) \frac{L}{3} \left[n_1(q) + 2n_2(q) \right] \dots (28)$$

where the geometrical thickness L is determined from the ground level population densities and the specified optical depth in Lyman α . T_i is the temperature of the ions and m_i is the mass of the ions. $n_1(q)$ and $n_2(q)$ are the population densities of level q at the edge and centre.

It was shown by Bates, Kingston and McWhirter (1962) that when the equations for an optically thin plasma are solved in terms of reduced variables, the

solution becomes independent of the ionic charge Z . The reduced variables are

$$\text{temperature} \quad \Theta = T_e/Z^2 \quad \dots (29)$$

$$\text{electron density} \quad \eta(c) = n(c)/Z^7 \quad \dots (30)$$

$$\text{population density} \quad \eta(p) = X n(p)/Z^{11} \quad \dots (31)$$

and their validity may be easily checked by substitution into the expressions for the various rate coefficients appearing in the optically thin equations.

Additional reduced variables are required for an optically thick plasma in which the intensities of lines are involved, and photo-excitation terms have to be included in the steady state equations.

The additional reduced variables are

$$\text{total line intensity} \quad \Sigma = \frac{I}{Z^9} \sqrt{\frac{M}{\Gamma}} \quad \dots (32)$$

$$\text{total radiated power} \quad \Pi = \frac{P}{Z^9} \sqrt{\frac{M}{\Gamma}} \quad \dots (33)$$

$$\text{geometrical size} \quad \Lambda = \frac{LZ^8}{X} \sqrt{\frac{M}{\Gamma}} \quad \dots (34)$$

where Γ relates the ion temperature T_i to the electron temperature T_e

$$T_i = \Gamma T_e \quad \dots (35)$$

and M is the mass of the ion m_i in terms of the mass of the hydrogen atom m_H

$$m_i = M m_H \quad \dots (36)$$

The optical depth in Lyman α is a specified independent variable which is independent of the ionic charge Z . This is true for the optical depths calculated in the other lines as well.

When the calculations are made with Z , X , Γ and M all set to unity, the actual variables of course equal the reduced variables.

The photo-excitation terms occur in the form

$$\frac{n(p)B(p,q)}{\sqrt{\pi}} \left(1 - \frac{\omega(p)n(q)}{\omega(q)n(p)} \right) \int_0^\infty \frac{\rho_\nu}{\Delta\nu_D} e^{-\left(\frac{\nu-\nu_0}{\Delta\nu_D}\right)^2} d\nu$$

where the term $1 - \frac{\omega(p)n(q)}{\omega(q)n(p)}$ includes the effect of stimulated emission and is dimensionless. The radiation density ρ_ν is obtained by integrating the intensity I_ν over all solid angles.

$$\rho_\nu = \frac{1}{c} \int_0^{4\pi} I_\nu d\omega \quad \dots (37)$$

and the intensity I_ν is calculated from the source function by solving the equation of transfer along a given direction.

$$I_\nu = e^{-\tau_\nu} \int_0^{\tau_\nu} f(\tau'_\nu) e^{\tau'_\nu} d\tau'_\nu \quad \dots (38)$$

The optical depth does not scale. The source function f is given by

$$f = \frac{c n(q)A(q,p)}{4\pi n(p)B(p,q)} \frac{1}{1 - \frac{n(q)\omega(p)}{n(p)\omega(q)}} \quad \dots (39)$$

which for a hydrogen-like ion of charge Z is proportional to Z^6 and so it follows that the intensity I_ν and radiation density ρ_ν are also proportional to Z^6 . In general the electron temperature and ion temperature will not be equal so that $\Delta\nu_D$ for a given transition may take any value, but the integral

$$\int_0^\infty \frac{\rho_\nu}{\Delta\nu_D} e^{-\left(\frac{\nu - \nu_0}{\Delta\nu_D}\right)^2} d\nu \quad \dots (40)$$

is independent of the value of $\Delta\nu_D$ and is also proportional to Z^6 . It is this property which makes the scaling laws possible for an optically thick plasma and when the other reduced variables are included it will be found that the steady state equations for an optically thick plasma also become independent of the ionic charge. This relationship is valid because the optical depth is regarded as an independent variable. When $\Delta\nu_D$ is altered, the optical depth of the plasma is not changed but the geometrical size is.

The accuracy of these calculations is determined by several factors. The actual cross sections used are probably only accurate to a factor of 3 and the effect of these will be the same as for the optically thin calculations. The accuracy of the solution of the equation of transfer has been discussed. For optical depths in Lyman α of 10 or less the error is less than 5%. The accuracy

of the solution at an optical depth of 100 is much less, about 30% and there is the additional error in the slow convergence of the equations which affects the ground level, so that the total error at an optical depth of 100 may be 50% or even a factor of 2. At low densities where levels 2 and 3 are populated directly from the ground level then the ratio of the intensities of Lyman α and β will not be affected by an error in the ground level.

It is assumed in these calculations that all the line profiles are dominated by Doppler broadening. As the electron density is increased the relative importance of Stark broadening will increase, but it is difficult to describe in general terms when Stark effect will have an important effect. At low electron densities where the ground level population is determined by radiative recombination, the Stark effect in the high levels will have no effect on the intensities of the lines emitted from the low levels which are populated by collisional excitation from the ground level. A criterion for the importance of Stark broadening for the Lyman α line of hydrogen was given in an earlier paper (Hearn 1963).

At higher electron densities the increasing Stark broadening of the lines is balanced in part by the increasing dominance of the collisional excitation and de-excitation processes over the radiative processes but a detailed solution of this problem has not been attempted.

Selected results for pure Doppler broadening are given in Table 1. The optical depth measured at the centre of Lyman α varies from 0.1 to 100 by factors of 10. The reduced electron density is in the range 10^8 to 10^{18} cm^{-3} and the reduced temperature from 8000 to 256000⁰K.

For each optical depth, electron density and temperature, the table gives the reduced intensity of the Lyman α and β lines and the Balmer α and β lines, the reduced geometrical size and the reduced total power loss by line radiation from the plasma.

The power loss by radiative recombination and bremsstrahlung, for which the plasma is optically thin, may be obtained from the calculations of McWhirter and Hearn (1963).

It is assumed in these calculations that the electron density and bare nuclei density, through the ratio X , are constant throughout the plasma. At low temperatures where the number density of bare nuclei is small compared with the number density of hydrogen-like ions the larger optical depths cause large variations in the ground level population density through the plasma which represents large variations in the total particle density. Because of this difficulty only optical depths of 0.1 and 1 are given for an electron temperature of 8000°K . Although it is quite easy to apply a conservation law to the total particle density for a specific plasma, of neutral hydrogen for example, the scaling laws with ionic charge would be lost. To illustrate the magnitude of the error and degree of ionization of the plasma for the low temperatures the ground level population density is given for the edge and centre of the plasma for temperatures of 8000 and 16000°K in Table 2 for reduced electron densities up to 10^{18} and for temperatures of $32,000$ and $64,000^{\circ}\text{K}$ for reduced electron densities up to 10^{12} . These tables should cover ionic charges up to 10.

TABLE 1a
The reduced intensity Σ of the Lyman α line
in ergs cm⁻² sec⁻¹ sterad⁻¹

$\eta(c)$	Θ	$\tau = 0.1$					
		8000	16000	32000	64000	128000	256000
$\leq 10^{14}$		$1.3^{-13} \eta(c)$	$2.4^{-10} \eta(c)$	$1.1^{-8} \eta(c)$	$8.9^{-8} \eta(c)$	$2.8^{-7} \eta(c)$	$6.0^{-7} \eta(c)$
10^{15}		1.2^2	2.1^5	9.0^6	6.2^7	1.8^8	3.6^8
10^{16}		6.7^2	1.3^6	6.0^7	4.4^8	1.2^9	2.2^9
10^{18}		1.3^3	3.1^6	1.8^8	1.8^9	8.8^9	2.9^{10}
		$\tau = 1.0$					
$\leq 10^{13}$		$1.8^{-12} \eta(c)$	$3.1^{-9} \eta(c)$	$1.5^{-7} \eta(c)$	$1.1^{-6} \eta(c)$	$3.8^{-6} \eta(c)$	$7.8^{-6} \eta(c)$
10^{14}		1.7^2	2.9^5	1.3^7	9.8^7	3.1^8	6.6^8
10^{15}		1.5^3	2.5^6	9.8^7	6.4^8	1.8^9	3.6^9
10^{16}		6.3^3	1.2^7	5.7^8	4.0^9	1.1^{10}	1.8^{10}
10^{18}		1.0^4	2.3^7	1.4^9	1.4^{10}	6.7^{10}	2.2^{11}
		$\tau = 10.0$					
$\leq 10^{12}$			$3.5^{-8} \eta(c)$	$1.6^{-6} \eta(c)$	$1.3^{-5} \eta(c)$	$4.4^{-5} \eta(c)$	$9.2^{-5} \eta(c)$
10^{13}			3.3^5	1.6^7	1.2^8	3.8^8	8.0^8
10^{14}			2.5^6	9.4^7	6.3^8	2.0^9	4.4^9
10^{15}			1.5^7	4.6^8	2.4^9	6.3^9	1.2^{10}
10^{16}			4.2^7	1.9^9	1.3^{10}	3.3^{10}	5.4^{10}
10^{18}			6.0^7	3.5^9	3.6^{10}	1.7^{11}	5.8^{11}
		$\tau = 100.0$					
$\leq 10^{11}$			$3.1^{-7} \eta(c)$	$1.5^{-5} \eta(c)$	$1.2^{-4} \eta(c)$	$3.7^{-4} \eta(c)$	$6.3^{-4} \eta(c)$
10^{12}			2.1^5	1.4^7	8.1^7	2.3^8	4.5^8
10^{13}			1.1^6	5.9^7	3.9^8	1.4^9	3.2^9
10^{14}			4.9^6	1.3^8	8.1^8	2.6^9	6.1^9
10^{15}			2.0^7	6.0^8	3.1^9	7.9^9	1.5^{10}
10^{16}			5.3^7	2.5^9	1.7^{10}	4.4^{10}	7.1^{10}
10^{18}			8.2^7	4.7^9	4.9^{10}	2.4^{11}	7.9^{11}

TABLE 1b
The reduced intensity Σ of the Lyman β line
in ergs cm⁻² sec⁻¹ sterad⁻¹

$\tau = 0.1$						
$\eta(c)$	Θ 8000	16000	32000	64000	128000	256000
$\leq 10^{13}$	$1.2^{-15} \eta(c)$	$9.0^{-12} \eta(c)$	$8.7^{-10} \eta(c)$	$9.7^{-9} \eta(c)$	$3.7^{-8} \eta(c)$	$8.3^{-8} \eta(c)$
10^{14}	1.9^{-1}	1.2^3	9.3^4	8.5^5	2.8^6	5.7^6
10^{15}	2.4^0	1.6^4	1.2^6	1.1^7	3.1^7	5.4^7
10^{16}	1.4^1	1.0^5	9.7^6	9.6^7	3.1^8	5.5^8
10^{18}	2.8^1	2.5^5	2.9^7	4.0^8	2.2^9	7.9^9
$\tau = 1.0$						
$\leq 10^{13}$	$1.3^{-14} \eta(c)$	$9.4^{-11} \eta(c)$	$9.1^{-9} \eta(c)$	$1.0^{-7} \eta(c)$	$3.9^{-7} \eta(c)$	$8.6^{-7} \eta(c)$
10^{14}	2.7^0	1.6^4	1.2^6	1.0^7	3.3^7	6.6^7
10^{15}	3.6^1	2.3^5	1.7^7	1.4^8	3.7^8	6.1^8
10^{16}	1.7^2	1.3^6	1.2^8	1.1^9	3.4^9	5.9^9
10^{18}	2.7^2	2.4^6	2.8^8	3.8^9	2.1^{10}	7.6^{10}
$\tau = 10$						
$\leq 10^{12}$		$8.2^{-10} \eta(c)$	$7.9^{-8} \eta(c)$	$9.0^{-7} \eta(c)$	$3.4^{-6} \eta(c)$	$7.7^{-6} \eta(c)$
10^{13}		1.5^4	1.2^6	1.3^7	4.9^7	1.1^8
10^{14}		3.6^5	2.0^7	1.5^8	4.4^8	8.9^8
10^{15}		3.9^6	2.2^8	1.4^9	3.4^9	5.3^9
10^{16}		1.2^7	1.0^9	9.3^9	2.7^{10}	4.4^{10}
10^{18}		1.6^7	1.8^9	2.5^{10}	1.4^{11}	4.9^{11}
$\tau = 100$						
$\leq 10^9$		$2.0^{-9} \eta(c)$	$2.0^{-7} \eta(c)$	$2.2^{-6} \eta(c)$	$8.4^{-6} \eta(c)$	$1.9^{-5} \eta(c)$
10^{10}		2.0^1	2.0^3	2.4^4	1.1^5	2.5^5
10^{11}		2.4^2	2.5^4	4.1^5	2.7^6	8.8^6
10^{12}		4.3^3	7.1^5	1.7^7	8.5^7	2.1^8
10^{13}		8.7^4	1.1^7	1.1^8	4.2^8	1.0^9
10^{14}		1.5^6	6.3^7	3.9^8	1.1^9	2.3^9
10^{15}		9.9^6	5.1^8	3.0^9	7.0^9	1.1^{10}
10^{16}		2.3^7	2.1^9	1.9^{10}	5.6^{10}	9.0^{10}
10^{18}		3.3^7	3.7^9	5.2^{10}	2.8^{11}	1.0^{12}

TABLE 1c
The reduced intensity Σ of the Balmer α line
in ergs cm⁻² sec⁻¹ sterad⁻¹

$\tau = 0.1$						
\leq	Θ 8000	16000	32000	64000	128000	256000
10^{12}	$1.6^{-16} \eta(c)$	$1.3^{-12} \eta(c)$	$1.4^{-10} \eta(c)$	$1.8^{-9} \eta(c)$	$7.6^{-9} \eta(c)$	$1.8^{-8} \eta(c)$
10^{13}	1.7^{-3}	1.3^1	1.3^3	1.6^4	6.5^4	1.5^5
10^{14}	2.5^{-2}	1.7^2	1.6^4	1.6^5	5.2^5	1.1^6
10^{15}	3.1^{-1}	2.6^3	2.7^5	2.9^6	8.1^6	1.2^7
10^{16}	1.9^0	1.8^4	2.4^6	3.5^7	1.5^8	2.8^8
10^{18}	3.7^0	4.2^4	7.0^6	1.3^8	7.9^8	3.0^9
$\tau = 1$						
10^{12}	$1.7^{-15} \eta(c)$	$1.3^{-11} \eta(c)$	$1.4^{-9} \eta(c)$	$1.7^{-8} \eta(c)$	$6.8^{-8} \eta(c)$	$1.6^{-7} \eta(c)$
10^{13}	2.1^{-2}	1.5^2	1.4^4	1.6^5	6.2^5	1.4^6
10^{14}	3.6^{-1}	2.4^3	2.0^5	1.8^6	5.6^6	1.1^7
10^{15}	5.0^0	3.9^4	3.7^6	3.3^7	8.0^7	1.1^8
10^{16}	2.3^1	2.2^5	2.6^7	2.6^8	8.1^8	1.4^9
10^{18}	3.7^1	4.2^5	5.5^7	4.8^8	1.8^9	5.7^9
$\tau = 10$						
10^{12}		$2.0^{-10} \eta(c)$	$2.2^{-8} \eta(c)$	$2.4^{-7} \eta(c)$	$9.6^{-7} \eta(c)$	$2.2^{-6} \eta(c)$
10^{13}		3.4^3	2.8^5	3.0^6	1.1^7	2.3^7
10^{14}		7.1^4	4.3^6	2.6^7	5.4^7	8.4^7
10^{15}		8.7^5	4.9^7	2.0^8	3.0^8	3.2^8
10^{16}		2.9^6	1.3^8	5.5^8	1.4^9	2.1^9
10^{18}		4.0^6	1.6^8	7.2^8	2.4^9	7.3^9
$\tau = 100$						
10^9		$5.6^{-9} \eta(c)$	$5.4^{-7} \eta(c)$	$6.0^{-6} \eta(c)$	$3.1^{-5} \eta(c)$	$8.6^{-5} \eta(c)$
10^{10}		5.6^1	5.5^3	6.3^4	3.4^5	1.0^6
10^{11}		6.0^2	6.0^4	8.2^5	5.3^6	1.8^7
10^{12}		5.2^3	1.0^6	2.0^7	7.5^7	1.6^8
10^{13}		1.1^5	8.2^6	4.4^7	9.7^7	1.7^8
10^{14}		1.2^6	3.4^7	8.4^7	1.3^8	1.8^8
10^{15}		8.8^6	1.3^8	3.4^8	4.6^8	4.7^8
10^{16}		2.0^7	2.0^8	7.2^8	1.7^9	2.7^9
10^{18}		2.4^7	2.2^8	8.8^8	2.9^9	8.5^9

TABLE 1d

The reduced intensity Σ of the Balmer β line
in ergs cm⁻² sec⁻¹ sterad⁻¹

$\tau = 0.1$

$\eta(c)$	Θ_{8000}	16000	32000	64000	128000	256000
$\leq 10^{11}$	$2.3^{-17} \eta(c)$	$2.8^{-13} \eta(c)$	$3.7^{-11} \eta(c)$	$5.1^{-10} \eta(c)$	$2.2^{-9} \eta(c)$	$5.0^{-9} \eta(c)$
10^{12}	2.2^{-5}	2.7^{-1}	3.5^1	4.6^2	1.9^3	4.5^3
10^{13}	2.6^{-4}	2.8^0	3.3^2	3.9^3	1.4^4	3.1^4
10^{14}	4.0^{-3}	4.3^1	4.6^3	4.7^4	1.4^5	2.5^5
10^{15}	5.2^{-2}	6.4^2	8.2^4	9.7^5	2.9^6	4.2^6
10^{16}	3.1^{-1}	4.4^3	7.0^5	1.2^7	5.6^7	1.1^8
10^{18}	6.3^{-1}	1.1^4	2.1^6	4.8^7	3.6^8	1.6^9

$\tau = 1$

$\leq 10^{11}$	$2.4^{-16} \eta(c)$	$2.9^{-12} \eta(c)$	$3.7^{-10} \eta(c)$	$4.8^{-9} \eta(c)$	$2.0^{-8} \eta(c)$	$4.5^{-8} \eta(c)$
10^{12}	2.4^{-4}	2.8^0	3.5^2	4.4^3	1.8^4	4.0^4
10^{13}	3.0^{-3}	3.2^1	3.5^3	3.8^4	1.4^5	3.0^5
10^{14}	5.8^{-2}	5.8^2	5.7^4	5.4^5	1.6^6	2.7^6
10^{15}	8.4^{-1}	9.7^3	1.1^6	1.2^7	3.3^7	4.5^7
10^{16}	3.9^0	5.7^4	8.6^6	1.3^8	5.5^8	1.0^9
10^{18}	6.3^0	1.1^5	2.0^7	3.9^8	2.3^9	8.5^9

$\tau = 10$

$\leq 10^{11}$		$3.7^{-11} \eta(c)$	$5.0^{-9} \eta(c)$	$6.2^{-8} \eta(c)$	$2.5^{-7} \eta(c)$	$5.7^{-7} \eta(c)$
10^{12}		3.6^1	4.7^3	5.8^4	2.3^5	5.3^5
10^{13}		5.9^2	5.4^4	5.9^5	2.1^6	4.6^6
10^{14}		1.7^4	1.3^6	9.2^6	2.3^7	3.6^7
10^{15}		2.2^5	2.0^7	1.5^8	3.2^8	3.7^8
10^{16}		7.7^5	9.5^7	8.1^8	2.4^9	4.0^9
10^{18}		1.1^6	1.5^8	1.2^9	4.6^9	1.4^{10}

$\tau = 100$

$\leq 10^{10}$		$1.1^{-9} \eta(c)$	$1.3^{-7} \eta(c)$	$1.6^{-6} \eta(c)$	$8.5^{-6} \eta(c)$	$2.4^{-5} \eta(c)$
10^{11}		1.1^2	1.3^4	1.7^5	1.0^6	3.3^6
10^{12}		6.8^2	1.6^5	3.8^6	1.7^7	4.1^7
10^{13}		1.8^4	1.7^6	1.6^7	4.6^7	8.5^7
10^{14}		2.9^5	1.7^7	7.9^7	1.3^8	1.7^8
10^{15}		2.6^6	1.5^8	5.7^8	8.7^8	8.7^8
10^{16}		7.4^6	3.2^8	1.4^9	3.6^9	6.0^9
10^{18}		9.7^6	3.6^8	1.7^9	6.0^9	1.8^{10}

TABLE 1e

The reduced total power π radiated by the lines
 from both sides in ergs $\text{cm}^{-2} \text{sec}^{-1}$

$\tau = 0.1$						
$\eta(c)$	Θ 8000	16000	32000	64000	128000	256000
$\leq 10^{12}$	$1.6^{-12} \eta(c)$	$2.9^{-9} \eta(c)$	$1.4^{-7} \eta(c)$	$1.2^{-6} \eta(c)$	$4.1^{-6} \eta(c)$	$8.8^{-6} \eta(c)$
10^{13}	1.6^1	2.9^4	1.4^6	1.2^7	3.9^7	8.3^7
10^{14}	1.6^2	2.9^5	1.4^7	1.1^8	3.6^8	7.4^8
10^{15}	1.4^3	2.7^6	1.3^8	1.0^9	3.0^9	5.6^9
10^{16}	7.9^3	1.7^7	9.4^8	8.0^9	2.5^{10}	4.6^{10}
10^{18}	1.6^4	3.9^7	2.8^9	3.3^{10}	1.7^{11}	6.0^{11}
$\tau = 1.0$						
$\leq 10^{12}$	$1.5^{-11} \eta(c)$	$2.8^{-8} \eta(c)$	$1.4^{-6} \eta(c)$	$1.2^{-5} \eta(c)$	$4.0^{-5} \eta(c)$	$8.5^{-5} \eta(c)$
10^{13}	1.5^2	2.8^5	1.4^7	1.2^8	3.9^8	8.1^8
10^{14}	1.5^3	2.8^6	1.3^8	1.1^9	3.4^9	7.0^9
10^{15}	1.3^4	2.5^7	1.2^9	9.1^9	2.5^{10}	4.6^{10}
10^{16}	5.7^4	1.3^8	7.7^9	6.4^{10}	1.9^{11}	3.4^{11}
10^{18}	9.0^4	2.4^8	1.8^{10}	2.2^{11}	1.1^{12}	4.0^{12}
$\tau = 10$						
$\leq 10^{12}$		2.3^{-7}	$1.2^{-5} \eta(c)$	$1.0^{-4} \eta(c)$	$3.5^{-4} \eta(c)$	$7.3^{-4} \eta(c)$
10^{13}		2.3^6	1.2^8	9.6^8	3.1^9	6.6^9
10^{14}		2.3^7	1.0^9	7.0^9	2.0^{10}	4.2^{10}
10^{15}		1.7^8	8.1^9	5.1^{10}	1.3^{11}	2.0^{11}
10^{16}		5.2^8	3.6^{10}	3.1^{11}	9.4^{11}	1.6^{12}
10^{18}		7.3^8	6.4^{10}	8.3^{11}	4.5^{12}	1.6^{13}
$\tau = 100$						
$\leq 10^{12}$		$1.9^{-6} \eta(c)$	$1.0^{-4} \eta(c)$	$8.7^{-4} \eta(c)$	$2.9^{-3} \eta(c)$	$5.7^{-3} \eta(c)$
10^{13}		9.3^6	6.0^8	4.3^9	1.4^{10}	3.1^{10}
10^{14}		8.9^7	3.5^9	2.0^{10}	4.9^{10}	8.8^{10}
10^{15}		5.5^8	2.8^{10}	1.7^{11}	3.9^{11}	5.8^{11}
10^{16}		1.3^9	1.0^{11}	9.8^{11}	3.0^{12}	5.1^{12}
10^{18}		1.8^9	1.7^{11}	2.4^{12}	1.3^{13}	4.9^{13}

TABLE 1f

The reduced geometrical size Λ of the plasma in cms

		$\tau = 0.1$					
$\eta(c)$	Θ	8000	16000	32000	64000	128000	256000
10^8		1.6^0	9.9^4	4.2^7	1.5^9	1.5^{10}	7.7^{10}
10^{11}		1.8^{-3}	1.1^2	4.5^4	1.5^6	1.5^7	7.8^7
10^{12}		2.1^{-4}	1.2^1	4.8^3	1.6^5	1.6^6	8.1^6
10^{13}		2.8^{-5}	1.5^0	5.7^2	1.9^4	1.8^5	8.9^5
10^{14}		4.5^{-6}	2.3^{-1}	8.3^1	2.6^3	2.3^4	1.1^5
10^{15}		5.9^{-7}	3.3^{-2}	1.3^1	4.0^2	3.6^3	1.7^4
10^{16}		3.5^{-8}	2.3^{-3}	1.0^0	3.6^1	3.6^2	1.9^3
10^{17}		6.5^{-10}	4.8^{-5}	2.5^{-2}	1.1^0	1.4^1	8.8^1
10^{18}		7.1^{-11}	5.4^{-7}	3.0^{-4}	1.4^{-2}	1.9^{-1}	1.4^0
		$\tau = 1$					
10^8		1.7^1	1.1^6	4.6^8	1.5^{10}	1.5^{11}	7.8^{11}
10^{11}		2.0^{-2}	1.2^3	4.8^5	1.6^7	1.5^8	7.9^8
10^{12}		2.3^{-3}	1.3^2	5.2^4	1.7^6	1.6^7	8.2^7
10^{13}		3.2^{-4}	1.7^1	6.2^3	2.0^5	1.8^6	9.1^6
10^{14}		6.3^{-5}	3.2^0	1.1^3	3.1^4	2.6^5	1.2^6
10^{15}		9.4^{-6}	5.0^{-1}	1.8^2	5.2^3	4.3^4	2.0^5
10^{16}		4.4^{-7}	2.9^{-2}	1.2^1	4.3^2	4.1^3	2.1^4
10^{17}		6.7^{-9}	5.0^{-4}	2.7^{-1}	1.2^1	1.4^2	9.2^2
10^{18}		7.1^{-11}	5.4^{-6}	3.0^{-3}	1.4^{-1}	1.9^0	1.4^1
		$\tau = 10$					
10^8		8.6^6	3.6^9	1.4^{11}	1.5^{12}	7.6^{12}	
10^{11}		9.5^3	3.9^6	1.5^8	1.5^9	7.8^9	
10^{12}		1.2^3	4.4^5	1.6^7	1.6^8	8.1^8	
10^{13}		2.5^2	8.0^4	2.3^6	2.0^7	9.7^7	
10^{14}		9.2^1	2.4^4	5.5^5	4.0^6	1.7^7	
10^{15}		1.2^1	3.3^3	7.8^4	5.9^5	2.5^6	
10^{16}		3.9^{-1}	1.7^2	5.4^3	4.9^4	2.4^5	
10^{17}		5.2^{-3}	2.8^0	1.2^2	1.5^3	9.6^3	
10^{18}		5.4^{-5}	3.0^{-2}	1.4^0	1.9^1	1.4^2	

TABLE 1f
(continued)

	$\tau = 100$				
$\eta(c)$	Θ_{16000}	32000	64000	128000	256000
10^8	6.3^7	2.6^{10}	9.4^{11}	1.2^{13}	5.7^{13}
10^{11}	7.6^4	3.0^7	1.0^9	1.1^{10}	5.4^{10}
10^{12}	7.5^3	5.0^6	1.4^8	1.2^9	5.5^9
10^{13}	4.8^3	1.6^6	4.0^7	3.0^8	1.2^9
10^{14}	1.5^3	3.4^5	7.1^6	5.0^7	2.1^8
10^{15}	1.4^2	3.9^4	8.9^5	6.4^6	2.7^7
10^{16}	4.1^0	1.8^3	5.9^4	5.2^5	2.4^6
10^{17}	5.3^{-2}	2.8^1	1.2^3	1.5^4	9.7^4
10^{18}	5.4^{-4}	3.0^{-1}	1.4^1	1.9^2	1.4^3

TABLE 2a

The reduced population density $\eta(1)$ for level 1 at
the edge and centre of the plasma

$\tau = 0.1$				
Θ	8000		16000	
$\eta(c)$	$\eta(1)$ centre	$\eta(1)$ edge	$\eta(1)$ centre	$\eta(1)$ edge
10^8	9.5^{11}	9.5^{11}	2.2^7	2.2^7
10^{11}	8.3^{14}	8.3^{14}	2.0^{10}	2.0^{10}
10^{12}	7.1^{15}	7.1^{15}	1.8^{11}	1.8^{11}
10^{13}	5.5^{16}	5.5^{16}	1.5^{12}	1.5^{12}
10^{14}	3.4^{17}	3.4^{17}	9.4^{12}	9.4^{12}
10^{15}	2.6^{18}	2.6^{18}	6.4^{13}	6.6^{13}
10^{16}	4.3^{19}	4.3^{19}	9.5^{14}	9.6^{14}
10^{17}	2.3^{21}	2.3^{21}	4.5^{16}	4.5^{16}
10^{18}	2.2^{23}	2.2^{23}	4.0^{18}	4.0^{18}

$\tau = 1.0$				
Θ	8000		16000	
$\eta(c)$	$\eta(1)$ centre	$\eta(1)$ edge	$\eta(1)$ centre	$\eta(1)$ edge
10^8	8.7^{11}	9.1^{11}	1.9^7	2.0^7
10^{11}	7.6^{14}	7.9^{14}	1.7^{10}	1.9^{10}
10^{12}	6.5^{15}	6.7^{15}	1.6^{11}	1.7^{11}
10^{13}	4.7^{16}	4.9^{16}	1.2^{12}	1.3^{12}
10^{14}	2.4^{17}	2.5^{17}	6.6^{12}	7.3^{12}
10^{15}	1.5^{18}	1.8^{18}	4.0^{13}	4.8^{13}
10^{16}	3.3^{19}	3.7^{19}	7.2^{14}	8.0^{14}
10^{17}	2.2^{21}	2.3^{21}	4.3^{16}	4.3^{16}
10^{18}	2.1^{23}	2.1^{23}	4.0^{18}	4.0^{18}

$\tau = 10.0$		
Θ	16000	
$\eta(c)$	$\eta(1)$ centre	$\eta(1)$ edge
10^3	2.1^7	3.2^7
10^{11}	1.9^{10}	2.9^{10}
10^{12}	1.6^{11}	2.3^{11}
10^{13}	7.5^{11}	1.0^{12}
10^{14}	1.6^{12}	3.8^{12}
10^{15}	1.3^{13}	3.0^{13}
10^{16}	4.8^{14}	7.0^{14}
10^{17}	4.0^{16}	4.3^{16}
10^{18}	4.0^{18}	4.0^{18}

TABLE 2a
(continued)

$\tau = 100.0$

Θ	16000	
$\eta(c)$	$\eta(1)$ centre	$\eta(1)$ edge
10^8	2.2^7	5.9^7
10^{11}	1.8^{10}	4.9^{10}
10^{12}	1.2^{11}	6.3^{11}
10^{13}	2.7^{11}	7.9^{11}
10^{14}	5.2^{11}	3.2^{12}
10^{15}	7.4^{12}	3.2^{13}
10^{16}	4.4^{14}	7.2^{14}
10^{17}	4.0^{16}	4.3^{16}
10^{18}	3.9^{18}	3.9^{18}

TABLE 2b

The reduced population density $\eta(1)$ for level 1 at
the edge and centre of the plasma

 $\tau = 0.1$

Θ	32,000		64,000	
	$\eta(1)$ centre	$\eta(1)$ edge	$\eta(1)$ centre	$\eta(1)$ edge
10^8	7.2^4	7.2^4	2.9^3	2.9^3
10^{11}	6.8^7	6.8^7	2.8^7	2.8^7
10^{12}	6.3^8	6.3^8	2.7^8	2.7^8

 $\tau = 1.0$

Θ	32,000		64,000	
	$\eta(1)$ centre	$\eta(1)$ edge	$\eta(1)$ centre	$\eta(1)$ edge
10^8	6.5^4	6.9^4	2.8^3	2.9^3
10^{11}	6.2^7	6.5^7	2.7^6	2.7^6
10^{12}	5.8^8	6.1^8	2.5^7	2.6^7

 $\tau = 10.0$

Θ	32,000		64,000	
	$\eta(1)$ centre	$\eta(1)$ edge	$\eta(1)$ centre	$\eta(1)$ edge
10^8	8.5^4	8.4^4	2.8^3	3.3^3
10^{11}	7.8^7	7.8^7	2.7^6	3.1^6
10^{12}	7.0^8	6.9^8	2.5^7	2.9^7

 $\tau = 100.0$

Θ	32,000		64,000	
	$\eta(1)$ centre	$\eta(1)$ edge	$\eta(1)$ centre	$\eta(1)$ edge
10^8	7.3^4	2.0^5	3.0^3	7.8^3
10^{11}	6.5^7	1.8^8	2.8^6	6.6^6
10^{12}	4.0^8	1.0^9	3.2^7	2.8^7

6. DISCUSSION OF THE RESULTS

The most interesting results of the calculation are the variation of the ratio of the intensity of the Lyman α and β lines emitted by the plasma and the variation of the ground level population density at the centre of the plasma with electron density and optical depth for a given electron temperature.

The variation of the decrement of Lyman β to Lyman α is shown in Fig.2 for an electron temperature of $16,000^{\circ}\text{K}$. The decrement is plotted against the optical depth in Lyman α for various electron densities.

For an optically thin plasma with a limitingly low density both levels 2 and 3 are populated directly from the ground level by means of electron excitation and depopulated by spontaneous transitions. The intensity in each line is proportional to the number of excitations to the upper level from the ground level. When the plasma becomes optically thick the effect of the optical thickness on the intensity is determined by the processes competing with the spontaneous transition probability to the ground level. If there are no competing processes the intensity of the line will grow linearly with optical depth as the total number of photons generated by electron excitation increases with the number of ground level atoms. The effect of competing processes has been discussed by Hearn (1964b). If all the competing processes are a fraction b of the spontaneous transition rate, then a fraction b of the photons will be lost each time a photon is absorbed and emitted. A photon is absorbed and emitted approximately τ times before reaching the edge of the plasma so that if

$$b\tau \ll 1 \quad \dots (41)$$

the intensity of the line increases linearly with optical depth. This region has been called effectively thin by Avrett and Hummer (1965). The main competing process for Lyman α radiation is usually electron excitation to level 3. For an electron temperature of $16,000^{\circ}\text{K}$ and an electron density of 10^8 cm^{-3} this is 10^7 times less likely than a spontaneous transition, so that the intensity of Lyman alpha clearly increases linearly in the range of optical depths considered

here for electron densities 10^8 cm^{-3} and higher and the variation of intensity is independent of the electron density.

The situation for Lyman β is quite different. The main process competing with the emission of a Lyman β photon is the emission of a Balmer α photon which leaves a low density plasma without being absorbed. So that at each absorption and emission of a photon a fraction

$$A(3,2)/[A(3,2) + A(3,1)]$$

which equals 0.44 is lost. As the optical depth increases, the intensity of Lyman β rapidly falls below the linear relation with optical depth and the decrement is reduced as Fig.2 shows. The effect of optical depth on both lines is independent of electron density since the departure from linearity of Lyman β is controlled only by spontaneous emission terms.

As the electron density increases, collisional excitation from level 3 to 4 becomes more important and at some stage would be a significant depopulating process for level 3 and decrease the decrement with increasing electron density. The calculations show however that before this happens, the mode of populating level 3 changes from collisional excitation from lower levels to collisional de-excitation and radiative cascade from higher levels and this has a far greater effect on the decrement, increasing it instead of decreasing it. At very high electron densities all the populations become collision dominated and the population densities are given by Local Thermodynamic Equilibrium. It is interesting to note that the smallest decrement for modest optical depths is given at low electron densities where there is a coronal regime of excitation.

The variation of the ground level population density at the centre of the plasma is shown in Fig.3 for an electron temperature of 16000°K . The population density is plotted against electron density for different optical depths.

For an optically thin plasma of limitingly low electron density the ground level is populated by radiative recombination to the bound levels followed by radiative cascade to the ground level. As the plasma becomes optically thick in

the lines, the radiative recombination to the ground level is not affected, and for moderate optical depths in Lyman α , the contribution to the ground level from radiative recombination to level 2 is not affected for the same reason given for the linear relation between the intensity of Lyman α and the optical depth, that is that an electron having arrived at level 2 eventually finds its way to the ground level with the loss from the plasma of a Lyman α photon. Only the contributions of radiative recombination to level 3 and above are affected by the optical thickness. But since the rate coefficient of radiative recombination to level p varies approximately as $1/p^3$ and the optical depth in the Lyman line from level p varies at a rate between $1/p^2$ and $1/p^3$ the effect of these upper levels is very small. An increase in the electron density increases the importance of collisional-radiative recombination; recombination by means of three-body recombinations at high bound levels followed by collisional de-excitation and radiative cascade. At the same time the population density of level 2 increases until the optical depth in Balmer α is significant. At these electron densities, radiative cascade is the dominant populating process of the ground level and photo-excitation in Balmer α has a significant effect on the ground level population which becomes sensitive to the optical thickness of the plasma in Balmer α . This is the region of slow convergence in the calculations, for the ground level population density calculated from a Holstein treatment in the Lyman lines does not include the effect of the Balmer α photo-excitation so that during the iteration the ground level population has to be altered by a large factor, and this is a slow process. The effect of Balmer α photo-excitation also makes the equations very non-linear so that it is not always possible to obtain a better starting value by including the effect of Balmer α photo-excitation by a Holstein treatment.

At high electron densities, the collision rates dominate all the radiative rates and the ground level population density goes to its Saha-Boltzmann value.

ACKNOWLEDGEMENTS

I am very grateful to Dr. R.W.P. McWhirter and Dr. R. Wilson for their comments and particularly for their encouragement without which this work would not have been done.

REFERENCES

- AMBARTSUMYAN, V.A., 1958, Theoretical Astrophysics (Oxford: Pergamon Press).
- AVRETT, E.H. and HUMMER, D.G., 1965, Mon. Not. R. Astr. Soc., 130, 295, (1965).
- BATES, D.R. and KINGSTON, A.E., 1963, Planetary and Space Science, 11, 1.
- BATES, D.R., KINGSTON, A.E. and McWHIRTER, R.W.P., 1962, Proc. Roy. Soc. A, 267, 297.
- BURGESS, A., 1961, Mem. Soc. Sci., Liege [5], 4, 299.
- GREEN, L.C., RUSH, P.P., and CHANDLER, C.D., 1957, Astrophys. J. (Suppl.), 3, 37.
- HEARN, A.G., 1963, Proc. Phys. Soc., 81, 648.
- HEARN, A.G., 1964a, Proc. Phys. Soc., 84, 11.
- HEARN, A.G., 1964b, Proc. VIth Int. Conf. Ionization Phenomena in Gases, Paris, 1963, 3, 289.
- HOLSTEIN, T., 1947, Phys. Rev., 72, 1212.
- HOLSTEIN, T., 1951, Phys. Rev., 83, 1159.
- McWHIRTER, R.W.P. and HEARN, A.G., 1963, Proc. Phys. Soc., 82, 641.
- SEATON, M.J., 1962, Atomic and Molecular Processes, Ed. D.R. Bates, (New York: Academic Press).
- THOMAS, R.N. and ATHAY, R.G., 1961, Physics of the Solar Chromosphere, (New York: Interscience Publishers, Inc.).
- UNSÖLD, A., 1955, Physik der Sternatmosphären, 2nd edn (Berlin: Springer-Verlag).

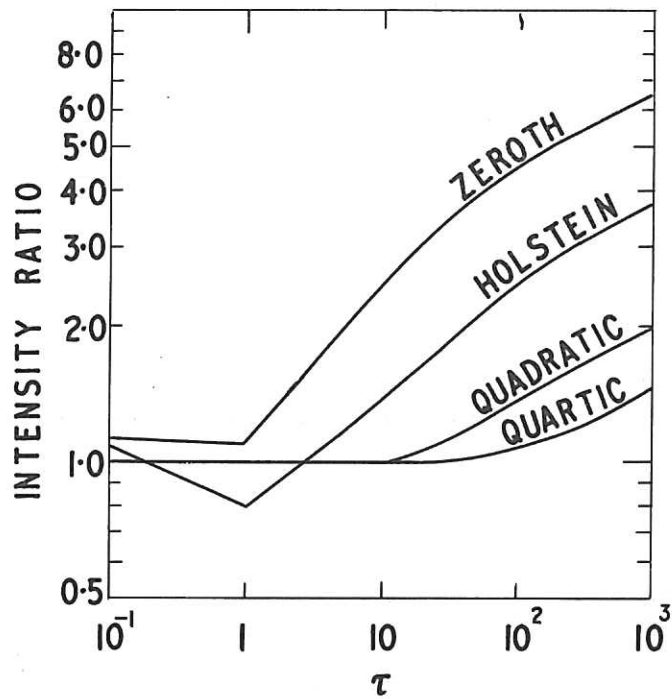


Fig. 1 (CLM-P 97)
 The total intensity of the line calculated using a zeroth, quadratic and quartic approximation for the source function and using Holstein's theory expressed as a ratio of the total intensity calculated using a 20th degree approximation for the source function plotted against optical thickness measured at the centre of the line for a limiting low electron density

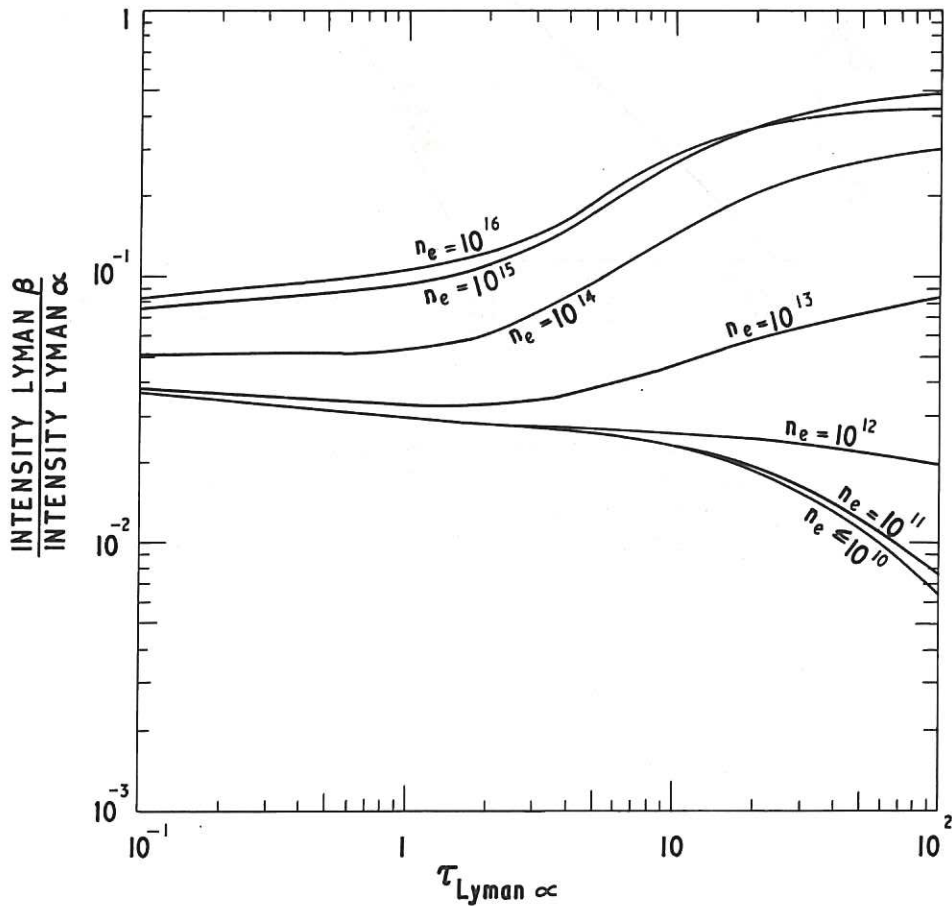


Fig. 2 (CLM-P 97)
 The ratio of the reduced total intensity of the Lyman β line to the Lyman α line plotted against optical thickness measured at the centre of the Lyman α line for various reduced electron densities for a reduced electron temperature of 16000°K

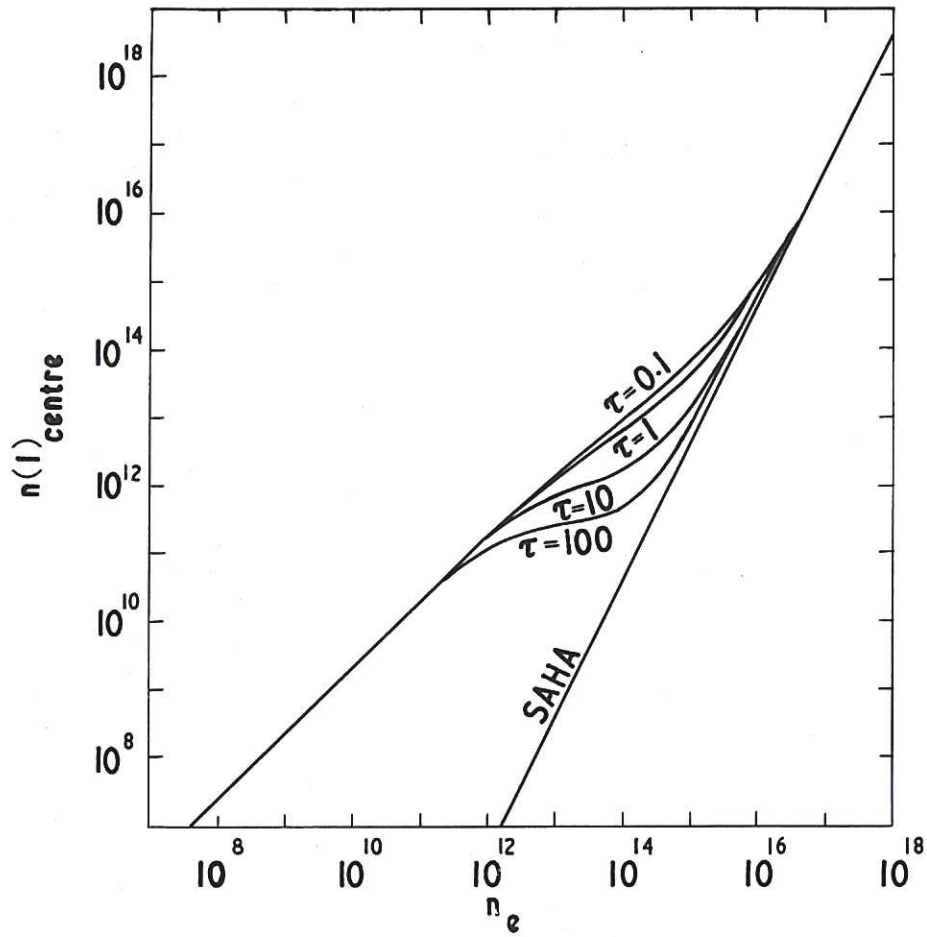


Fig. 3

(CLM-P 97)

The reduced ground level population density at the centre of the plasma plotted against the reduced electron density for various optical thicknesses measured at the centre of the Lyman α line and for the Saha-Boltzmann distribution for a reduced electron temperature of 16000 $^{\circ}$ K

